

In the format provided by the authors and unedited.

## Imaging and tuning polarity at SrTiO<sub>3</sub> domain walls

Yiftach Frenkel<sup>1</sup>, Noam Haham<sup>1</sup>, Yishai Shperber<sup>1</sup>, Christopher Bell<sup>2</sup>, Yanwu Xie<sup>3,4,5</sup>, Zhuoyu Chen<sup>5</sup>, Yasuyuki Hikita<sup>3</sup>, Harold Y. Hwang<sup>3,5</sup>, Ekhard K.H. Salje<sup>6,7</sup> and Beena Kalisky<sup>1,\*</sup>

1. Department of Physics and Institute of Nanotechnology and Advanced Materials, Bar-Ilan University, Ramat-Gan, 5290002, Israel

2. H. H. Wills Physics Laboratory, University of Bristol, Tyndall Avenue, Bristol, BS8 1TL, UK

3. Stanford Institute for Materials and Energy Sciences, SLAC National Accelerator Laboratory, Menlo Park, California 94025, USA

4. Department of Physics, Zhejiang University, Hangzhou, 310027, China

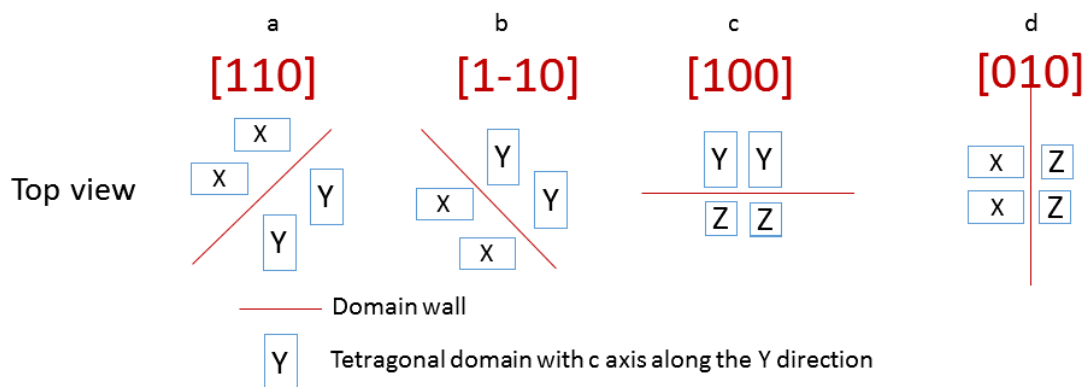
5. Department of Applied Physics, Geballe Laboratory for Advanced Materials, Stanford University

476 Lomita Mall, Stanford University, Stanford, California, 94305, USA

6. Department of Earth Sciences, University of Cambridge, Downing Street, Cambridge CB2 3EQ, United Kingdom

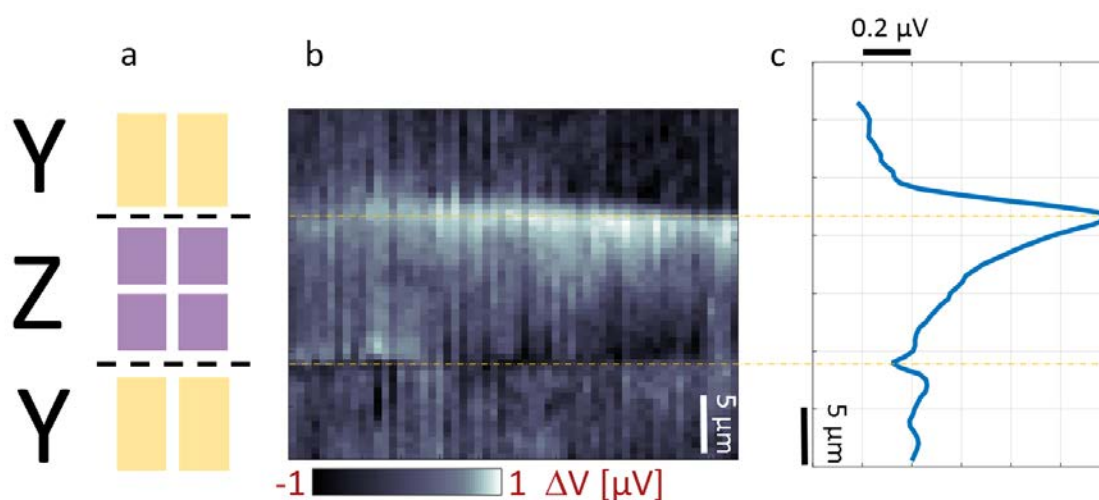
7. State Key Lab Mech. Behav. Mat., Xi'an Jiaotong University, Xi'an 710049, China

\* beena@biu.ac.il



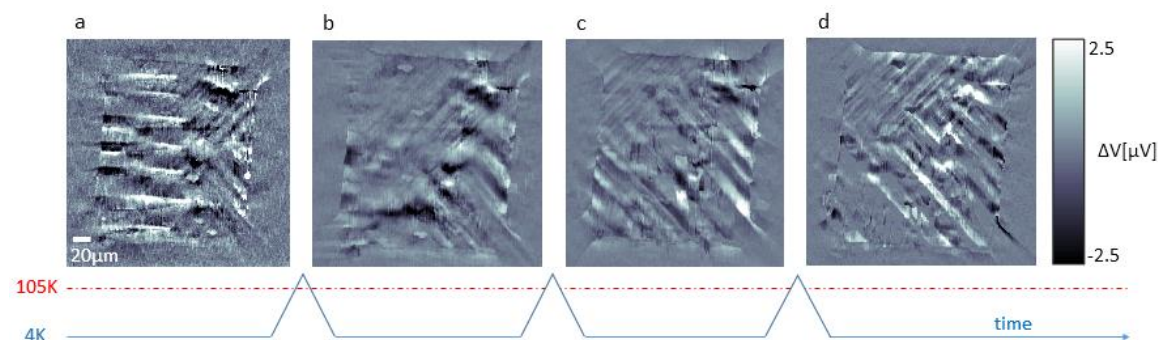
### Supplementary Figure S1 | Direction of domain walls

The direction of the domain wall depends on its adjacent domains. The illustration shows the different possible orientation of domain walls. An intersection between in plane domains will result in either [110] or [1-10] domains (a-b). An intersection between in plane and out of plane domains (X,Y and Z) will result in a domain wall directed either along [100] (Y and Z) or along [010] (X and Z) (c-d). In this manner it is possible to know which are the domains adjacent to the wall, but it is impossible to distinguish between them.



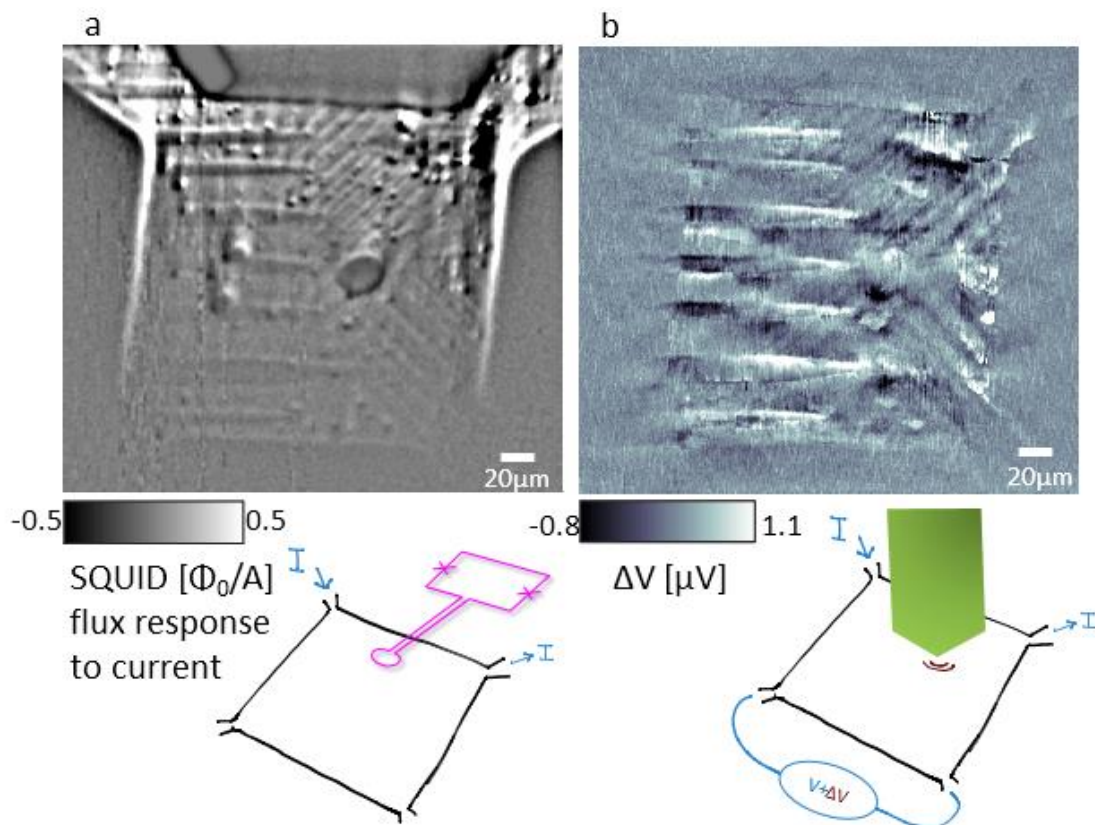
### Supplementary Figure S2 | Scanning over the domain walls

As the tip moves from a Y domain into a Z domain we can see a small negative response. And as the tip goes from Z to Y, we can see a much bigger positive response (i.e. an increase in the resistance of the sample). The axes of the image are in pixels, with each pixel being 0.5  $\mu\text{m}$ . Note: it is known that the domain wall is between Z and Y domains but it is not possible to determine which one is Z and which is Y. Their order was chosen arbitrarily. (a) Illustration, the interface between Y and Z (or Z and Y) domains results in [100] walls. (b)  $\Delta V$  data. Two sharp signal lines in the [100] direction are observed when scanning over the [100] domain walls. These lines indicate an abrupt change in the polarization of the walls. (c) A line cut across the [100] walls shows a smaller negative peak at the first wall and then a larger positive peak at the second.



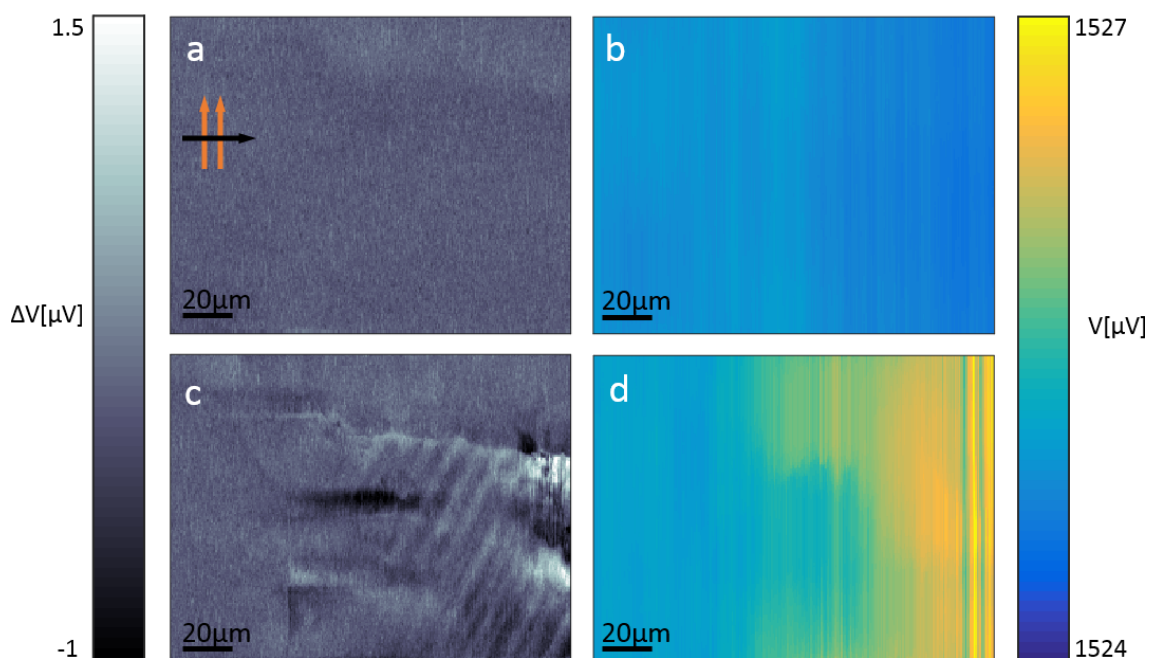
### Supplementary Figure S3 | Different domain configurations

(a-d)  $\Delta V$  images, each image was obtained at 4.2K after the sample temperature was raised to above 105K and re-cooled. This figure demonstrates that after each temperature cycle around the 105 K cubic to tetragonal transition, a new domain configuration is formed. We use this experiment to correlate the stripes observed in  $\Delta V$  with the STO tetragonal domains.



### Supplementary Figure S4 | Mapping current flow with scanning SQUID microscopy

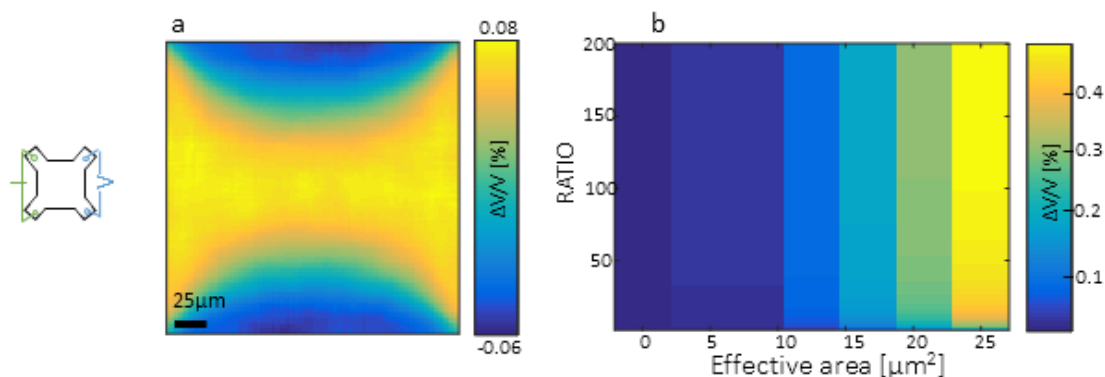
(a) Scanning SQUID maps of local current flow, known to be modulated on STO domain structure in LAO/STO,<sup>10,11</sup> illustrates the same configuration of stripes as the  $\Delta V$  map recorded simultaneously. (b) The main difference between the images is that the current flow image concentrates on the areas of stronger current flow - mostly between the current leads. Areas away from the leads are weaker in the image.  $\Delta V$ , the four probe voltage, highlights the entire square and follows the hourglass shape described in Fig. 3 in the main text. Cartoons below the figures describe the way the measurements are made, with scanning SQUID microscopy (below panel a) and scanning stress microscopy (below panel b).



### Supplementary Figure S5 | Time dependent component of the signal

In addition to  $\Delta V$ , we observed a time-dependent component. It appears as line noise, but it is related to stress on the sample, since it is never observed when we press outside the sample. The signal of the time-dependent component is comparable to  $\Delta V$ .

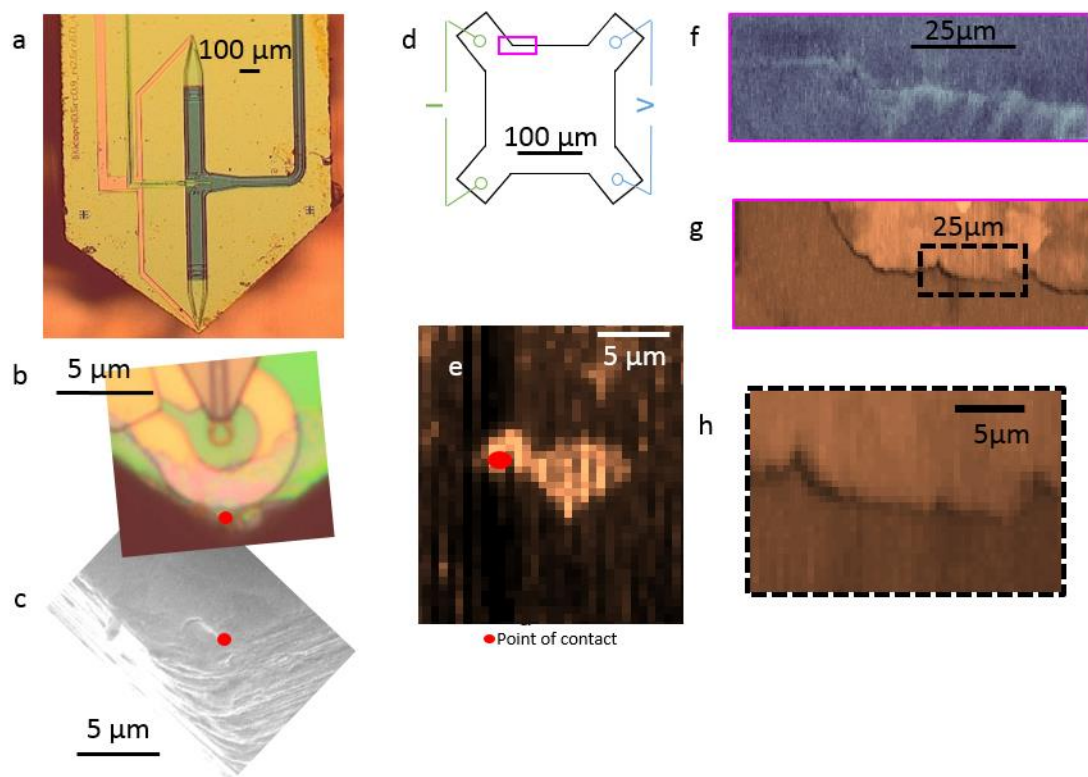
(a)  $\Delta V$  signal, recorded with very light contact ( $\sim 0.01 \mu\text{N}$ ) with the sample. Only a relatively weak signal was observed. Orange and black arrows indicate fast and slow scanning direction (line time is 18 seconds). (b) Background voltage (time-dependent signal); no significant voltage drift was observed during the scan. (c)  $\Delta V$  signal shows clear domain wall response with stronger pressing force ( $0.54 \mu\text{N}$ ). (d) Background signal showing strong time-dependent component with stronger press. The background signal only appears when the tip scans over the sample.



### Supplementary Figure S6 | $\Delta V$ calculation in response to local change in conductivity.

(a) We calculated the global response to a local change in resistivity. We found that the global change in voltage ( $\Delta V$ ) as a function of location of the resistivity change has an hourglass shape. (b) At a specific location we calculated  $\Delta V$  for different parameters.  $\Delta V$  increases with the ratio of resistivity change, and also increases with the area of resistivity change (effective contact area). The diagram shows that in order to obtain values that are similar to the data (0.17%) we need an effective area of contact that is at least  $15\mu\text{m}^2$ . Y-axis: ratio between values of resistivity, before and after we changed the resistivity of an effective area. X-axis: effective contact area, the size of the area for which we changed the resistivity. The calculations are detailed below:

We solved  $\nabla \cdot (\sigma \nabla V) = 0$  for  $V$ , where  $\sigma$  is the sample conductivity, which we chose to be isotropic and uniform ( $\sigma = 1$ , in arbitrary units,  $au$ ). We introduced the effect of pressure by the tip as a change (reduction) of the conductivity in a small area, equivalent to the area of the contact point ( $<1\mu\text{m}^2$ ). Changing the local conductivity redistributes the current flow in the sample. The voltage difference is the sum of the current  $\times (1/\sigma)$  at each pixel along the edge between the voltage corners, and therefore more current means a commensurately larger voltage drop. The calculated  $\Delta V$  is the difference in voltage (calculated between the corners of the device) between the modified local conductivity (as a result of tip pressing the sample) and the case of homogeneous conductivity. The difference is expressed as a percentage of the homogeneous case.



### Supplementary Figure S7 | Estimating the stress kernel of our tip

(a) Optical image of the scanning SQUID chip. (b) Zoom in on the sharpened tip of the SQUID chip, showing the contact point. (c) SEM image of the tip of the SQUID. (d) Illustration of the measurements setup. Note that because of the shape and relatively blunt tip we can only reach this resolution for sharp separated features that are perpendicular to the scanning direction. (e) Surface sensing. Here we scanned over a sharp feature in order to visualize the shape of our tip. Image of the sharpened edge of the SQUID's chip shown in (b). (f)  $\Delta V$  and (g) surface sensing signal of the pink area in (d), a sharp signal can be seen as the tip scans over the top edge of the sample. (h) Zoom in on the dotted square in (g), a  $\sim 1.5 \mu\text{m}$  line can be seen indicating our resolution. The images a-c are of a similar SQUID to the one used in this work.